

JPET #257717

Title page

**Radiosensitizing effect of novel phenylpyrimidine derivatives on human lung cancer
cells via cell cycle perturbation**

Seung-Youn Jung, Ky-Youb Nam, Jeong-In Park, Kyung-Hee Song, Jiyeon Ahn, Jong Kuk Park,
Hong-Duck Um, Sang-Gu Hwang, Sang Un Choi and Jie-Young Song*

Division of Radiation Biomedical Research, Korea Institute of Radiological & Medical Sciences,
Seoul 01812, Republic of Korea. (S.-Y. J., J.-I. P., K.-H. S., J. A., J. K. P., H.-D. U., S.-G. H., J.-Y. S.)

Research Center, Pharos I&BT Co., Ltd., Anyang 14059, Republic of Korea. (K.-Y. N.)

Graduate School of Pharmaceutical Sciences, College of Pharmacy, Ewha Womans University, Seoul
03760, Republic of Korea. (K.-H. S.)

Bio & Drug Discovery Division, Korea research Institute of Chemical Technology, Daejeon 34114,
Republic of Korea. (S. U. C.)

JPET #257717

Running Title page

Running Title: **Radiosensitizing effect of novel phenylpyrimidine compound**

***Address correspondence to:** Jie-Young Song, Division of Radiation Biomedical Research, Korea Institute of Radiological & Medical Sciences, 75 Nowon-ro, Nowon-gu, Seoul 01812, Republic of Korea. Tel.: +82 29701308; Fax: +82 29702402; E-mail address: immu@kirams.re.kr

Number of text pages: 26

Number of tables: 3

Number of figures: 4

Number of references: 45

Number of words in the *Abstract*: 224

Number of words in the *Introduction*: 387

Number of words in the *Discussion*: 1397

Non-standard Abbreviations:

CDK, Cyclin-dependent kinase; DMSO, dimethyl sulfoxide; MTT, 3-(4,5-dimethylthiazol-2-yl)-2,5-diphenyltetrazolium bromide; PARP, poly (ADP-ribose) polymerase; PBS, phosphate-buffered saline; PI, propidium iodide; PPA, N-phenylpyrimidin-2-amine; RT, radiotherapy; γ H2AX, gamma H2A histone family member X

Recommended section assignment:

Chemotherapy, Antibiotics, and Gene Therapy

JPET #257717

Abstract

Radiotherapy is one of the most common treatments for cancer, but radioresistance and injury to normal tissue are considered major obstacles to successful radiotherapy. Thus, there is an urgent need to develop radiosensitizers to improve the therapeutic outcomes of radiotherapy in cancer patients. Our previous efforts to identify novel radiosensitizers, using high-throughput screening targeting p53 and Nrf2 revealed a promising N-phenylpyrimidin-2-amine (PPA) lead compound; 17 derivatives of this lead compound were examined in the present study. PPA5, 13, 14, 15, and 17 inhibited cell viability by more than 50% with a marked increase in the proportion of cells arrested at the G2/M phase of cell cycle. Among these compounds, PPA15 markedly increased the sub-G1 cell population and increased the levels of cyclin B1 and the phosphorylation levels of cyclin-dependent kinases 1 (CDK1). Combined treatment with radiation and PPA14 or PPA15 significantly decreased clonogenic survival. An *in vitro* kinase assay revealed that PPA15 inhibited multiple CDKs involved in cell cycle regulation. Compared with drug or radiation treatment alone, combined treatment with PPA15 and radiation resulted in the suppression of A549 tumor growth in mice by 59.5% and 52.7%, respectively. Treatment with PPA15 alone directly inhibited tumor growth by 25.7%. These findings suggest that the novel pan CDK inhibitor, PPA15, may be a promising treatment to improve the effectiveness of radiotherapy for the treatment of cancer.

Significance Statement (<120 words)

Several inhibitors of CDK have been successfully evaluated in combination with other chemotherapeutics in clinical trials, but negative side effects have partially restricted their clinical use. In this study, we identified a novel pan-CDK inhibitor to increase radiosensitivity, and we hope this work will encourage the development of promising small-molecule radiosensitizers.

Introduction

Radiotherapy (RT) is used to treat up to 50% of cancer patients, making it the most common therapeutic strategy for cancers treatment (Chi *et al.*, 2018). However, a considerable number of patients undergoing radiotherapy develop radioresistance and experience recurrence, with a consequent deterioration of the prognosis and a decreased survival rate. Recent advances in molecular and cellular biology have revealed that several diverse factors play a role in the acquisition of radioresistance in human cancers: the number and intrinsic radiosensitivity of cancer stem cells, tumor hypoxia and reoxygenation during treatment, repopulation between radiotherapy fractions and redistribution of surviving cells, and DNA damage repair (Petersen *et al.*, 2001; Yaromina *et al.*, 2011; Krause *et al.*, 2011; Baumann *et al.*, 2016; Sharma *et al.*, 2016). Therefore, the development of effective radiation response modifiers that target the above-described relevant pathways is extremely important for increasing the efficacy of radiotherapy (Harrington *et al.*, 2011).

Cyclin-dependent kinases (CDKs) are a family of serine-threonine kinases that play a critical role in cell cycle regulation (CDK1, 2, 4, and 6), transcriptional regulation (CDK7, 8, and 9), and neuronal function (CDK5) (Asghar *et al.*, 2015). Aberrations in CDKs, affecting cell cycle control and their cyclin partners, have been observed in various cancers, usually characterized by dysregulated cell division (Malumbres and Barbacid, 2001). Thus, CDKs have long been regarded as attractive targets for the development of pharmacological inhibitors for cancer treatment. Many early, first-generation, non-selective CDK inhibitors showed toxicity and poor efficacy; however, the recent development of multi-target CDK inhibitors and more selective targeting of CDK4/6 inhibitors has led to the approval of palbociclib for the treatment of breast cancer (O'Leary *et al.*, 2016; Sherr *et al.*, 2016).

In our attempts to identify novel radiosensitizers, we performed cell-based screening using a luciferase-reporter assay system targeting tumor protein 53 (p53; TP53), nuclear factor (erythroid-derived 2)-like 2 (Nrf2; NFE2L2), and transforming growth factor beta (TGF- β) (Lim *et al.*, 2012; Kang *et al.*, 2015; Lee *et al.*, 2012; Jung *et al.*, 2015). A chemical library of 14,600 compounds was screened, and we identified a hit compound containing an aniline-pyrimidine scaffold, as shown in

JPET #257717

Table 1. These chemotypes are known to be promiscuous kinase inhibitors and have been heavily patented. Therefore, in this study, we synthesized several derivatives of the hit compound and determined their biological activities and underlying mechanisms.

Materials and methods

General methods for chemistry

All reactions involving air-sensitive reagents were performed in an inert atmosphere (N₂ or Ar) using syringe-septum cap techniques. All glassware was oven-dried prior to use. Mass spectra were recorded on a JMS-700 MStation (EI mode; JEOL Ltd., Tokyo, Japan). The ¹H NMR spectra were recorded on an Avance-500 (Bruker Daltonics Inc. Billerica, MA, USA). Chemical shifts are expressed as δ values relative to trimethylsilyl as the internal standard, J values are expressed in Hz, and spectra were recorded in CDCl₃ or hexadeuterodimethyl sulfoxide (DMSO-d₆; Sigma-Aldrich, St. Louis, MO, USA). Multiplicities of signals are indicated by the following symbol: s (singlet), d (doublet), dd (double doublet), t (triplet), m (multiplet) and brs (broad singlet). All reagents used were acquired from Sigma-Aldrich and used without further purification unless otherwise stated. The N-phenylpyrimidin-2-amine (PPA) compounds PPA1–PPA8 were purchased from ChemBridge (San Diego, CA, USA).

4-(4-fluorophenyl)-N-(4-nitrophenyl)pyrimidin-2-amine (PPA9)

¹H NMR (DMSO-d₆, 400 MHz): δ = 10.5 (1H, s), 8.68 (1H, d, J = 4.0 Hz), 8.52 (1H, s), 8.23-8.32 (3H, m), 8.10 (2H, d, J = 8.0 Hz), 7.62 (1H, d, J = 8.0 Hz), 7.42 (2H, t, J = 8.0 Hz). Mass (FAB⁺): m/z 311.1 (MH⁺). Yellow solid.

4-(4-fluorophenyl)-N,6-diphenylpyrimidin-2-amine (PPA10)

¹H NMR (DMSO-d₆, 400 MHz): δ = 9.75 (1H, s), 8.38-8.42 (2H, m), 8.32-8.34 (2H, m), 8.00 (1H, s), 7.91 (2H, d, J = 8.0 Hz), 7.57-7.59 (3H, m), 7.42 (2H, t, J = 10.0 Hz), 7.35 (2H, t, J = 8.0 Hz), 6.99 (1H, t, J = 8.0 Hz). Mass (FAB⁺): m/z 342.1 (MH⁺). Yellow solid.

N-(4-((4-(4-Fluorophenyl)pyrimidin-2-yl)amino)phenyl)acetamide (PPA11)

JPET #257717

¹H NMR (CDCl₃, 400 MHz): δ = 8.35-8.40 (3H, m), 7.54 (2H, d, J = 8.0 Hz), 7.37 (2H, d, J = 12.0 Hz), 7.18 (1H, brs), 7.13 (2H, t, J = 8.0 Hz), 6.75 (1H, brs), 6.53 (1H, d, J = 8.0 Hz), 2.20 (3H, s). Mass (FAB⁺): m/z 323.1 (MH⁺). Yellow solid.

4-(4-fluorophenyl)-N-(4-(4-methylpiperazin-1-yl)phenyl)pyrimidin-2-amine (PPA12)

¹H NMR (CDCl₃, 400 MHz): δ = 8.35-8.41 (2H, m), 8.30 (1H, d, J = 4.0 Hz), 7.24-7.28 (2H, m), 7.13 (2H, t, J = 8.0 Hz), 6.97 (2H, d, J = 8.0 Hz), 6.68 (1H, brs), 6.45 (1H, d, J = 4.0 Hz), 3.23 (4H, t, J = 6.0 Hz), 2.60 (4H, d, J = 6.0 Hz), 2.37 (3H, s). Mass (FAB⁺): m/z 364.2 (MH⁺). Yellow solid.

4-((4-(4-fluorophenyl)pyrimidin-2-yl)amino)-3-methoxy-N-methyl-benzamide (PPA13)

¹H NMR (CDCl₃, 400 MHz): δ = 8.35-8.41 (2H, m), 8.30 (1H, d, J = 4.0 Hz), 7.24-7.28 (2H, m), 7.13 (2H, t, J = 8.0 Hz), 6.97 (2H, d, J = 8.0 Hz), 6.68 (1H, brs), 6.45 (1H, d, J = 4.0 Hz), 3.23 (4H, t, J = 6.0 Hz), 2.60 (4H, d, J = 6.0 Hz), 2.37 (3H, s). Mass (FAB⁺): m/z 353.1 (MH⁺). Yellow solid.

4-((4-(4-fluorophenyl)pyrimidin-2-yl)amino)benzenesulfonamide (PPA14)

¹H NMR (DMSO-d₆, 400 MHz): δ = 10.1 (1H, s), 8.62 (1H, d, J = 4.0 Hz), 8.26 (2H, dd, J = 10.0, 4.0 Hz), 7.99 (2H, d, J = 8.0 Hz), 7.77 (2H, d, J = 8.0 Hz), 7.52 (1H, d, J = 4.0 Hz), 7.41 (2H, t, J = 10.0 Hz), 7.19 (2H, s). Mass (FAB⁺): m/z 345.1 (MH⁺). Bright yellow solid.

4-((4-(2-chlorophenyl)pyrimidin-2-yl)amino)benzenesulfonamide (PPA15)

¹H NMR (DMSO-d₆, 400 MHz): δ = 10.2 (1H, s), 8.66 (1H, d, J = 8.0 Hz), 7.96 (2H, d, J = 8.0 Hz), 7.72 (2H, d, J = 8.0 Hz), 7.62-7.69 (2H, m), 7.52-7.56 (2H, m), 7.20 (1H, d, J = 4.0 Hz), 7.28 (2H, s). Mass (FAB⁺): m/z 361.0 (MH⁺). Yellow solid.

4-(2-chlorophenyl)-N-(3-nitrophenyl)pyrimidin-2-amine (PPA16)

¹H NMR (DMSO-d₆, 400 MHz): δ = 10.3 (1H, s), 8.95 (1H, s), 8.69 (1H, d, J = 4.0 Hz), 8.08-8.15

JPET #257717

(1H, m), 7.79-7.81 (1H, m), 7.70-7.73 (1H, m), 7.63-7.66 (1H, m), 7.52-7.59 (3H, m), 7.24 (1H, d, $J = 4.0$ Hz). Mass (FAB⁺): m/z 327.1 (MH⁺). Green solid.

4-((4-(2-chlorophenyl)pyrimidin-2-yl)amino)-N-methylbenzamide (PPA17)

¹H NMR (DMSO-d₆, 400 MHz): $\delta = 10.0$ (1H, s), 8.64 (1H, d, $J = 8.0$ Hz), 8.21-8.26 (1H, m), 7.87 (2H, d, $J = 12.0$ Hz), 7.76 (2H, d, $J = 8.0$ Hz), 7.62-7.68 (2H, m), 7.51-7.54 (2H, m), 7.16 (1H, d, $J = 4.0$ Hz), 2.75 (3H, d, $J = 4.0$ Hz). Mass (FAB⁺): m/z 339.1 (MH⁺). White solid.

Cell culture and treatment

Human lung carcinoma A549 and H1299 cells, prostate carcinoma DU 145 cells, ovarian carcinoma SKOV3 cells, glioblastoma U-87 MG cells, and breast cancer MDA-MB-231 cells were purchased from the American Type Culture Collection (ATCC, Manassas, VA, USA). The cells were grown in RPMI 1640 or Dulbecco's modified Eagle's medium (Welgene, Daegu, Korea) supplemented with 10% fetal bovine serum, 100 IU/ml penicillin, and 100 μ g/ml streptomycin (Invitrogen, Carlsbad, CA, USA). Cells were maintained at 37°C in a humidified atmosphere containing 5% CO₂. All compounds were dissolved in DMSO and the final concentration of DMSO did not exceed 0.1% (v/v). All controls were treated with DMSO only.

Cell viability assay

Cell viability was evaluated with the 3-(4,5-dimethylthiazol-2-yl)-2,5-diphenyltetrazolium bromide (MTT; Sigma-Aldrich) colorimetric growth assay. Briefly, cells were seeded in 96-well plates at a density of 1,000 cells/well and treated with the indicated compounds for 72 h. All tested substances were dissolved in DMSO and diluted to the indicated final test concentrations. MTT (5 mg/ml) was added to the cells, and they were further incubated for 4 h at 37°C. The supernatant was removed, 100 μ l DMSO was added, and then the absorbance was measured at 540 nm using a microplate reader (Multiskan EX; Thermo Fisher Scientific, Waltham, MA, USA). All experiments were performed in

JPET #257717

triplicate.

Apoptosis assay

Apoptosis was evaluated by measuring the proportion of annexin-positive cells. Cells were labeled with allophycocyanin-conjugated annexin V and propidium iodide (PI) in binding buffer (BD Biosciences, San Diego, CA, USA) according to the manufacturer's instructions and analyzed using a FACSCalibur™ Flow Cytometer (BD Biosciences). For each sample, at least 10,000 events/sample were acquired. The percentage of annexin V-APC-positive cells was analyzed with FlowJo software V 7.2.5 (Tree Star Inc., Ashland, OR, USA).

Cell cycle analysis

A549 cells were seeded in 6-well plates at a density of 10,000 cells/cm² and treated under the indicated conditions. Cells were harvested and fixed in 75% ethanol for 1 h. They were then washed with phosphate-buffered saline (PBS) and resuspended in PBS buffer containing 100 µg/ml RNase A (Sigma-Aldrich) and 50 µg/ml PI, followed by incubation at 37 °C for 30 min. A minimum of 10,000 events/sample were analyzed by flow cytometry to determine the DNA content. The percentage of singlet cells in each cell cycle stage (sub-G1, G0/G1, S, G2/M, or aneuploid) was analyzed with FlowJo software V 7.2.5.

Clonogenic assay

Cell survival after irradiation was determined using a clonogenic assay (Dunne *et al.*, 2003). Briefly, cells were seeded on 60-mm tissue culture dishes at various densities, treated with the indicated compounds at 1 µM for 24 h, and then exposed to 3 or 3.5 Gy radiation with a ¹³⁷Cs gamma irradiator (BioBeam 8000; Gamma-Service Medical GmbH, Leipzig, Germany). After 10-14 days, colonies were fixed and stained with 1.0% methylene blue in absolute methanol solution for 10 min. Colonies larger than 0.1 mm diameter were scored as surviving colonies. The experiment was performed in

JPET #257717

triplicate for each cell line.

Kinase assays

The activity of each compound, at a concentration of 10 μM and with an ATP concentration of 10 μM , was screened against a protein kinase panel of 106 human protein kinases provided by the Eurofins' KinaseProfiler™ Service (Eurofins Pharma Discovery Services, Dundee, UK). The half-maximal inhibitory concentration (IC_{50}) values were calculated from 10-point dose-response curves provided by the Eurofins IC_{50} Profiler™ Service.

Western blot analysis

Total proteins from each cell lines was extracted in TNN buffer (50 mM Tris-Cl, pH 7.4; 1% NP-40; 150 mM NaCl, and 1 mM EDTA) supplemented with protease inhibitors (1 mM phenylmethylsulfonyl fluoride, 1 $\mu\text{g/ml}$ aprotinin, 1 $\mu\text{g/ml}$ leupeptin, and 1 mM Na_3VO_4) and quantified using the Bradford method. Protein samples (15 μg) were separated by SDS-PAGE and transferred to a nitrocellulose membrane. After blocking the non-specific antibody binding sites, the membrane was incubated overnight at 4 °C with specific antibodies against p-cdc25C (S216) (63F9; Cell Signaling Technology, Billerica, MA, USA), cdc25C (5H9; Cell Signaling), p-CDK2 (T160) (Cell Signaling Technology, Billerica, MA, USA), CDK2 (78B2; Cell Signaling), p-cdc2 (p-CDK1) (Y15) (10A11; Cell Signaling), cdc2 (PHO1; Cell Signaling), p-Histone H3 (p-HH3) (S10) (D2C8; Cell Signaling), Histone H3 (HH3) (Cell Signaling), Cyclin A2 (BF683; Cell Signaling), Cyclin B1 (D5C10; Cell Signaling), p53 (DO-1; Santa Cruz Biotechnology, Santa Cruz, CA, USA), p21 Waf/Cip1 (12D1; Cell Signaling), gamma H2A histone family member X (γH2AX ; Santa Cruz Biotechnology), poly (ADP-ribose) polymerase (PARP) (46D11; Cell Signaling), and β -actin (Sigma-Aldrich). After incubation with peroxidase-conjugated secondary antibodies at 37°C for 1 h, the protein bands were visualized using enhanced chemiluminescence reagent (GE Healthcare Biosciences, Pittsburgh, PA, USA) and detected using the Amersham Imager 680 (GE Healthcare

JPET #257717

Biosciences). The relative levels of phosphorylated protein expression were normalized by to their correspondent total protein and the relative levels of other protein expression were normalized to β -actin.

Tumor xenograft mouse models

Female 6-week-old athymic nude (nu/nu) mice from Orient Bio Inc. (Seongnam, Korea) were housed under specific pathogen-free conditions in microisolator cages with laboratory chow and water *ad libitum*. A549 cell xenografts were established by implanting 1×10^6 cultured cells subcutaneously into the thigh of the right hind leg of the mice. The tumor site was locally irradiated with 5 Gy ^{60}Co γ -radiation (2 Gy/min) when the tumor volumes reached 100–150 mm³. PPA5 (10 mg/kg) or PPA15 (2 mg/kg) was administered intraperitoneally 3 h before irradiation. The tumor was measured along two axes (L, longest axis; W, shortest axis) with Vernier calipers two or three times per week after irradiation. Tumor volume was calculated as $(L \times W^2)/2$ (mm³). All animal experiments were approved by the Institutional Animal Care and Use Committees (IACUC) of the Korea Institute of Radiological & Medical Sciences (KIRAMS 2018-0031).

Statistical analysis

Statistical analyses were performed using GraphPad software version 5 (GraphPad, La Jolla, CA, USA). All data are expressed as the mean \pm standard deviation (SD), except for the xenograft assay, where data are expressed as the mean \pm standard error (SE). Significant differences between groups were determined using analysis of variance (ANOVA) and Bonferroni post-hoc comparisons. A value of $P < 0.05$ was considered statistically significant.

JPET #257717

Results

Chemistry

The structures of the PPA derivatives are shown in Table 1. PPA1–PPA8 were purchased from ChemBridge, and the new PPA derivatives (PPA9–PPA17) were synthesized according to the methods outlined in Scheme 1.

Effects of PPA derivatives on cell viability

The MTT assay was used to evaluate the *in vitro* cell viability after incubation with each compound at a fixed concentration of 10 μ M in A549 human lung cancer cells. Compared to the DMSO control, compounds PPA4, PPA5, and PPA13–PPA17 displayed > 50% growth inhibition after 72 h (Fig. 1A). To investigate the inhibitory effect of these compounds on cell growth, asynchronously growing A549 cells were exposed to each compound for 72 h and cell cycle analysis was performed (Supplemental Table 1). As shown in Fig. 1B, PPA5, and PPA13–PPA17 significantly increased the population of cells in G2/M. In addition, the population of aneuploidy cells with an abnormal number of chromosomes (> 4n) (Orr *et al.*, 2015; Pantazi *et al.*, 2014) was also increased following treatment with these five compounds, except PPA5. PPA14 induced the most evident arrest at the G2/M phase, with 72.4% of the cell population in G2/M; only 9.0% of cells treated with PPA14 were in the G0/G1 phase compared to 78.4% of cells in the DMSO control. In addition, PPA15 significantly increased the proportion of cells in the sub-G1 phase, an indicator of cell death, from 1.5% in control cells to 9.8% (Fig. 1C).

Radiosensitizing effect of PPA derivatives

Among the tested PPA derivatives, we selected six compounds (PPA5, and PPA13–PPA17) for further investigation based on the above findings. Since highly proliferative cancer cells are more susceptible to chemotherapy or radiotherapy during G2/M arrest (Guha, 2012), we aimed to determine whether

JPET #257717

the selected PPA compounds would increase the sensitivity of cancer cells to radiation. Consistent with many earlier findings, irradiation alone increased the proportion of cells in the G2/M phase from 15.2% in the DMSO control to 41.1% (Supplemental Table 2). PPA5, PPA16, and PPA17 treatment in conjunction with irradiation additively increased the population of cells in G2/M arrest after 48 h, whereas treatment with PPA13–PPA15 alone caused a large population of cells to remain in the G2/M phase. Given the results of Fig. 1C, G2/M arrest induced by each PPA5, PPA16, and PPA17 was maintained for 72 h, while PPA13–PPA15-induced G2/M arrest occurred early, and released slowly. Interestingly, an increase in the sub-G1 cell population was observed only with a combination of PPA15 and irradiation, suggesting that PPA15 may be the most effective radiosensitizer compound (Fig. 2A and Supplemental Table 2). To further confirm the radiosensitizing effect of the selected compounds, we measured clonogenic survival, which is the most reliable and classical method to determine radiosensitivity (Buch *et al.*, 2012). As shown in Fig. 2B and 2C, treatment with PPA13, PPA14, and PPA15 alone increased the cytotoxicity of the cells. Moreover, the radiation-induced clonogenic survival of A549 human lung carcinoma cells showed a greater decrease following treatment with PPA14 or PPA15, suggesting that both these compounds possess radiosensitizing activity.

PPA derivatives induce G2/M arrest

To further investigate the molecular mechanism underlying the induction of G2/M arrest by the selected PPA derivatives, we measured the levels of proteins involved in G2/M phase progression in p53 wild-type A549 and p53-null H1299 cells. PPA15 and PPA16 treatment increased the levels of phosphorylated cdc25c (S216) in A549 cells, which is a suppressed state of cdc25c phosphatase function and thus prevents cell progression from G2 to mitosis. In addition, increased levels of active CDK2 (T160), inhibitory CDK1 (Y15), cyclin A2, and cyclin B1 expression by PPA14 and PPA 15 in both cell lines indicated that cells remained primarily in the G2 phase. In particular, the treatment of PPA14, PPA15, and PPA17 significantly decreased expression of phosphorylated histone-H3,

JPET #257717

indicating that the cells did not enter the mitotic phase or already exited the mitotic phase. The levels of p53 in A549 cells were increased by some PPAs, while p21 expression was highly increased in H1299 cells by PPA14 and PPA15 treatment. These results indicate that PPA15 effectively increased the proportion of cells in the G2/M phase by modifying the activity of the cyclin/CDK complex in a p53 independent manner.

Anti-tumor effect of PPA

To further evaluate the radiosensitivity of PPA15, we measured apoptotic cell death in the presence or absence of p53 function. As shown in Fig. 4A, combined treatment with PPA15 and irradiation significantly increased the population of annexin-positive cells in a p53 independent manner. It is well-known that p53 and p21 are key regulators of cell cycle arrest and apoptosis, and that both are involved in G1 as well as G2/M arrest after irradiation, thereby sensitizing tumor cells to radiation (Iliakis *et al.*, 2003; Jung *et al.*, 2017). As expected, irradiation markedly increased the protein levels of p53 and p21 in p53 wild-type A549 cells, whereas PPA15 did not significantly alter p53/p21 levels, but rather increased the levels of PARP1 cleavage and γ H2AX expression. In p53-null H1299 cells, p21 levels were slightly increased in response to both irradiation and PPA15, either alone or in combination. In addition, PARP1 cleavages and γ H2AX levels were also increased in the same treatment (Fig. 4B). These data suggest that PPA15 may effectively increase radiation-induced cell death via cell cycle perturbation with insufficient DNA damage repair.

Based on these results, the weakest (PPA5) and most active (PPA15) compounds were selected for the evaluation of anti-tumor effects in an *in vivo* xenograft mouse model. Mice were administered with 10 mg/kg PPA5 or 2 mg/kg PPA15 intraperitoneally 3 h prior to local irradiation. The body weights of the mice during the whole experiment did not differ significantly between all groups. Compared to the control, PPA5 alone, radiation alone, and combined PPA5 and irradiation treatment inhibited tumor growth by 14.7%, 36.5%, and 70.9%, respectively (Fig. 4C). PPA15 treatment at 20% that for PPA5 resulted in 25.7% tumor inhibition compared to control levels. PPA15 in combination

JPET #257717

with irradiation inhibited tumor growth more effectively than PPA15 alone or radiation alone, but a synergistic effect was not observed. Despite the insignificant effect on radiosensitivity by PPA15 in the animal study, the clonogenic survival of several irradiated cancer cells, including DU 145 prostates, SKOV3 cervical, U-87 glioma, and MDA-MB-231 breast cancer cells, was significantly decreased by PPA15 at 1 μ M (Fig. 4E, Supplemental Fig. 1), suggesting the usefulness of PPA15 as an adjuvant for radiotherapy, with broad activity across multiple tumor types.

To identify the target molecule of PPA15, we performed an *in vitro* kinase assay. In contrast to the non-specificity of PPA5, PPA15 showed highly selective inhibition of CDK/cyclin complexes (Table 2). PPA15 majorly inhibited the kinase activity of p25/CDK5, cyclin E/CDK2, cyclin E/CDK3, and cyclin A/CDK2 (IC_{50} , 9, 12, 18, and 19 nmol/L, respectively) and was less active against cyclin B/CDK1 or cyclin D/CDK4 by at least several-fold (Table 3).

Discussion

Although RT is a crucial and cost-effective strategy for the clinical treatment of cancer (Sharma *et al.*, 2016), its curative effect is not totally reliable. The need to improve the therapeutic outcomes of radiotherapy gives rise to an urgent requirement for the discovery and clinical application of new radiosensitizer drugs. The results of the present study indicate that PPA15 shows great potential as an effective radiosensitizer, via cell cycle perturbation, for use in human cancer treatment.

The cell cycle is inextricably linked to the cellular response to radiation. Radiation-induced single or double strand DNA breaks trigger multiple signaling pathways, including DNA damage responses and the activation of cell cycle checkpoints (Johnson and Shapiro, 2010). In addition, cells in the G2/M phase of the cell cycle are approximately three-times more radiosensitive than cells in the S phase (Terasima and Tolmach, 1963). Furthermore, many cancer cells have mutations or deletions in the *p53* gene or other *p53* signaling pathway defects that impair its role in controlling G1 checkpoint, which leads to a far greater reliance on G2 checkpoints than that observed in normal cells (Kawabe, 2004). Therefore, novel compounds could exert radiosensitizing activity by increasing the proportion of tumor cells in a more radiosensitive cell cycle phase (Pauwels *et al.*, 2010). The *p53* tumor suppressor protein plays a key role in numerous signaling pathways, including those involved in DNA repair, cell cycle progression, redox systems, inflammation, senescence, apoptosis, and metabolism (Fei and El-Deiry, 2003; Levine and Oren, 2009). The PPA moiety was identified by performing cell-based high-throughput screening to identify novel small molecules that increase radiosensitivity via *p53* modulation (Kang *et al.*, 2015). Among the 17 derivatives of PPA investigated, 6 were selected based on their ability to inhibit cell viability and induce G2/M arrest.

The combined treatment of the selected compounds with irradiation more strongly induced G2/M arrest than each compound alone, except for PPA15, which stimulated the release of cells from arrest and reentry into the cell cycle. Clonogenic survival analysis of the selected compounds demonstrated that PPA15 was the most effective radiosensitizer. Since distinctive G2/M arrest was observed in

JPET #257717

response to PPA compounds, we examined their effect on the expression of cell cycle-related proteins in two cell lines with different p53 status. The treatment-induced decrease in cyclin A/CDK2 and increase in cyclin B/CDK2 levels allowed cells to enter the G2 phase. Concomitantly, inhibitory cdc25c and CDK1 levels were increased, suggesting that cells were arrested in M phase without p53 dependency. In addition, the rapid release from G2/M arrest by PPA15 and irradiation treatment may have induced cell death, as evidenced by the increase in the apoptotic cell population, PARP1 cleavage and γ H2AX levels. Finally, the administration of a single dose of PPA15 (2 mg/kg) significantly inhibited tumor growth in mice. However, the *in vivo* radiosensitizing effect of PPA15 was weakly observed in this study. Because the effect of candidate compounds *in vivo* is highly dependent on experimental conditions, optimal PPA15 regimens, including dose, routes of administration, and schedule of the combined irradiation will likely vary for different types of tumors and will have to be determined accordingly. In addition, further pharmacokinetic/pharmacodynamic analysis of PPA15 is required to obtain maximum efficacy.

According to the kinase inhibitory profile of PPA15, most CDK/cyclin complexes were inhibited by PPA15. Thus, PPA15 is considered as a pan-CDK inhibitor (IC_{50} values for CDK1, CDK2, CDK3, CDK5, and CDK9 were in the 10–100 nM range). The underlying functions of CDK3 and CDK5 are currently unclear. CDK3 is intrinsically important for the entry of cells into the S phase via activation of transcription factors belonging to the E2F family, but its role can be readily compensated by other CDKs (Ye *et al.*, 2001). CDK5 was largely considered a neuronal kinase that protected the nervous system from damage. However, it was recently demonstrated that CDK5 has functions similar to those of CDK4 and CDK2 in driving cell cycle progression from G1 to S in medullary thyroid cancer models (Pozo *et al.*, 2013). CDK9 is involved in basal transcriptional regulation via the phosphorylation of RNA polymerase II and plays a crucial role in cell growth, proliferation, and differentiation (Romano and Giordano, 2008).

CDKs are highly validated targets for cancer therapeutics because they play a critical role in the regulation of cell cycle checkpoints and transcription. CDKs are major drug targets, and many CDK

JPET #257717

inhibitors have been described in the literature. However, because of the functional redundancy of CDKs/cyclins and their critical roles in normal cellular growth, pharmaceutical strategies to develop multiple-targeting or broad-spectrum CDK inhibitors remains limited, and are being pursued in parallel (Satyanarayana and Kaldis, 2009). Redundant CDKs can easily compensate for the loss of another's function in cancer cells, which provides an acceptable therapeutic margin via differences of their activity in normal cells versus cancer cells (Syn et al., 2018). Therefore, it would be anticipated that simultaneously targeting a range of CDKs is more likely to be therapeutically effective than the selective inhibition of specific CDKs. To date, optimized pan-CDK inhibitors or multi-target CDK inhibitors have been extensively investigated, and some clinical benefits have been demonstrated. However, numerous CDK inhibitors have shown disappointing results in clinical trials, possibly owing to an insufficient understanding of their mechanism of action, the absence of biomarkers, and the resulting inappropriate patient selection (Whittaker et al., 2017). Elucidation of the critical targets of these multi-target inhibitors could allow us to better determine the most effective strategy for deploying these agents in a clinical setting (Garrett and Collins, 2011).

Several studies have demonstrated that CDK2, CDK4, and CDK6 are not essential for cell cycle regulation in normal cells (Kozar and Sicinski, 2005; Dean et al., 2010; Sawai et al., 2012). However, CDK1 is known to be required for mammalian cell proliferation, and appears to be a key determinant in stimulating the onset of mitosis (Santamaría et al., 2007). Therefore, inhibitors that target CDK1 frequently lack selectivity for cancer cells over normal tissues, and cause problematic effects such as bone marrow suppression, as well as other adverse effects commonly associated with traditional chemotherapy, such as nausea, vomiting, and diarrhea (Asghar et al., 2015). For example, the use of Dinaciclib (MK-7965), which inhibits CDK1, 2, 5, and 9, has been attempted in patients with leukopenia and thrombocytopenia (Kumar et al., 2015; Mitri et al., 2015). The clinical development of the CDK1, 2, and 9 inhibitor AZD5438 was discontinued partially because of its low tolerability and high variability in patients (Boss et al., 2010; Prevo et al., 2018). Targeted individual CDK inhibitors could protect normal cells against some cancers, but might have therapeutic value against restricted

JPET #257717

tumors showing the expression and activation of these specific CDKs. Nevertheless, selective CDK4/6 inhibitors (Palbociclib, Ribociclib, Abemaciclib) have been licensed for the treatment of hormone receptor–positive, retinoblastoma–positive breast cancer in combination with antihormonal agents (Hamilton and Infante, 2016). Based on new findings that non-cell cycle-related CDKs are associated with cancer in diverse ways, selective inhibitors of CDKs 5, 7, 8, 9, and 12 have been developed. Moreover, alternative approaches to discovering allosteric sites, protein-protein interactions, and peptidomimetic mechanisms are also underway to overcoming the selectivity problem for ATP-competitive agents (Heptinstall et al., 2018).

The narrow therapeutic window of CDK-targeted inhibitors remains a huge obstacle to effective treatment; nevertheless, certain drugs with an in correct range of CDK selectivity as well as the combination of CDK1 inhibitors with other targeted therapies continue to be developed (Whittaker *et al.*, 2017; Xia *et al.*, 2014; Wu *et al.*, 2018). Many studies have suggested that CDK inhibitors often do not lead to tumor shrinkage, especially in solid tumors, but rather result in greater cytotoxic effects when used in combination with other chemotherapeutics or radiotherapy (Guha, 2012). Consistent with the above findings, PPA15 alone directly decreased the tumor volume in A549 xenograft mice, suggesting that it is a promising agent for cancer treatment, either alone or as part of a combination therapy. DNA-damaging chemotherapeutic agents combined with radiotherapy is common treatment strategy, but many concerns still needed to be addressed, including optimizing scheduling, appropriate target selection, improved preclinical models, and biomarker-based patient selection.

In conclusion, PPA15 treatment induced cell cycle arrest at the G2/M phase and enhanced the radiosensitivity of cancer cells via the inhibition of CDK1, CDK2, CDK3, and CDK5. Further studies are needed to establish the optimal sequence and schedule of PPA15 administration in combination with radiotherapy.

JPET #257717

Authorship Contributions

SY Jung and KY Nam contributed equally to this work.

Conducted experiments: SY Jung, KH Song, and JI Park.

Performed data analysis: SY Jung, KH Song, and JI Park.

Performed drug design and synthesized compounds: KY Nam.

Interpreted the data: J Ahn, HD Um, JK Park, and SG Hwang.

Wrote or contributed to the writing of the manuscript: SY Jung, KY Nam, SU Choi, and JY Song.

Supervised the research design and laboratory activities: JY Song.

References

- Asghar U, Witkiewicz AK, Turner NC, and Knudsen ES (2015) The history and future of targeting cyclin-dependent kinases in cancer therapy. *Nat Rev Drug Discov* **14**:130–146.
- Baumann M, Krause M, Overgaard J, Debus J, Bentzen SM, Daartz J, Richter C, Zips D, and Bortfeld T (2016) Radiation oncology in the era of precision medicine. *Nat Rev Cancer* **16**:234–249.
- Boss DS, Schwartz GK, Middleton MR, Amakye DD, Swaisland H, Midgley RS, Ranson M, Danson S, Calvert H, Plummer R, Morris C, Carvajal RD, Chirieac LR, Schellens JHM, and Shapiro GI (2010) Safety, tolerability, pharmacokinetics and pharmacodynamics of the oral cyclin-dependent kinase inhibitor AZD5438 when administered at intermittent and continuous dosing schedules in patients with advanced solid tumours. *Ann Oncol Off J Eur Soc Med Oncol* **21**:884–894.
- Buch K, Peters T, Nawroth T, Sanger M, Schmidberger H, and Langguth P (2012) Determination of cell survival after irradiation via clonogenic assay versus multiple MTT Assay--a comparative study. *Radiat Oncol Lond Engl* **7**:1.
- Chi H-C, Tsai C-Y, Tsai M-M, and Lin K-H (2018) Impact of DNA and RNA Methylation on Radiobiology and Cancer Progression. *Int J Mol Sci* **19**:555-578.
- Dean JL, Thangavel C, McClendon AK, Reed CA, and Knudsen ES (2010) Therapeutic CDK4/6 inhibition in breast cancer: key mechanisms of response and failure. *Oncogene* **29**:4018–4032.
- Dunne AL, Price ME, Mothersill C, McKeown SR, Robson T, and Hirst DG (2003) Relationship between clonogenic radiosensitivity, radiation-induced apoptosis and DNA damage/repair in human colon cancer cells. *Br J Cancer* **89**:2277–2283.
- Fei P, and El-Deiry WS (2003) P53 and radiation responses. *Oncogene* **22**:5774–5783.
- Garrett MD and Collins I (2011) Anticancer therapy with checkpoint inhibitors: what, where and when? *Trends Pharmacol Sci* **32**:308-316.
- Guha M (2012) Cyclin-dependent kinase inhibitors move into Phase III. *Nat Rev Drug Discov*

JPET #257717

11:892–894.

Hamilton E and Infante JR (2016) Targeting CDK4/6 in patients with cancer. *Cancer Treat Rev* **45**:129-138.

Harrington KJ, Billingham LJ, Brunner TB, Burnet NG, Chan CS, Hoskin P, Mackay RI, Maughan TS, Macdougall J, McKenna WG, Nutting CM, Oliver A, Plummer R, Stratford IJ, and Illidge T (2011) Guidelines for preclinical and early phase clinical assessment of novel radiosensitisers. *Br J Cancer* **105**:628–639.

Heptinstall AB, Adiyasa I, Cano C and Hardcastle IR (2018) Recent advances in CDK inhibitors for cancer therapy. *Future Med Chem* **10**:1369-1388.

Iliakis G, Wang Y, Guan J, and Wang H (2003) DNA damage checkpoint control in cells exposed to ionizing radiation. *Oncogene* **22**:5834–5847.

Johnson N, and Shapiro GI (2010) Cyclin-dependent kinases (cdks) and the DNA damage response: rationale for cdk inhibitor-chemotherapy combinations as an anticancer strategy for solid tumors. *Expert Opin Ther Targets* **14**:1199–1212.

Jung S-Y, Kho S, Song K-H, Ahn J, Park I-C, Nam K-Y, Hwang S-G, Nam S-Y, Cho S-J, and Song J-Y (2017) Novel focal adhesion kinase 1 inhibitor sensitizes lung cancer cells to radiation in a p53-independent manner. *Int J Oncol* **51**:1583–1589.

Jung S-Y, Yi JY, Kim M-H, Song K-H, Kang S-M, Ahn J, Hwang S-G, Nam K-Y, and Song J-Y (2015) IM-412 inhibits the invasion of human breast carcinoma cells by blocking FGFR-mediated signaling. *Oncol Rep* **34**:2731–2737.

Kang MA, Kim M-S, Kim JY, Shin Y-J, Song J-Y, and Jeong J-H (2015) A novel pyrido-thienopyrimidine derivative activates p53 through induction of phosphorylation and acetylation in colorectal cancer cells. *Int J Oncol* **46**:342–350.

Kawabe T (2004) G2 checkpoint abrogators as anticancer drugs. *Mol Cancer Ther* **3**:513–519.

Kozar K, and Sicinski P (2005) Cell cycle progression without cyclin D-CDK4 and cyclin D-CDK6 complexes. *Cell Cycle Georget Tex* **4**:388–391.

JPET #257717

- Krause M, Yaromina A, Eicheler W, Koch U, and Baumann M (2011) Cancer stem cells: targets and potential biomarkers for radiotherapy. *Clin Cancer Res Off J Am Assoc Cancer Res* **17**:7224–7229.
- Kumar SK, LaPlant B, Chng WJ, Zonder J, Callander N, Fonseca R, Fruth B, Roy V, Erlichman C, Stewart AK, and Mayo Phase 2 Consortium (2015) Dinaciclib, a novel CDK inhibitor, demonstrates encouraging single-agent activity in patients with relapsed multiple myeloma. *Blood* **125**:443–448.
- Lee S, Lim M-J, Kim M-H, Yu C-H, Yun Y-S, Ahn J, and Song J-Y (2012) An effective strategy for increasing the radiosensitivity of Human lung Cancer cells by blocking Nrf2-dependent antioxidant responses. *Free Radic Biol Med* **53**:807–816.
- Levine AJ, and Oren M (2009) The first 30 years of p53: growing ever more complex. *Nat Rev Cancer* **9**:749–758.
- Lim M-J, Ahn J-Y, Han Y, Yu C-H, Kim M-H, Lee S-L-O, Lim D-S, and Song J-Y (2012) Acriflavine enhances radiosensitivity of colon cancer cells through endoplasmic reticulum stress-mediated apoptosis. *Int J Biochem Cell Biol* **44**:1214–1222.
- Malumbres M, and Barbacid M (2001) To cycle or not to cycle: a critical decision in cancer. *Nat Rev Cancer* **1**:222–231.
- Mitri Z, Karakas C, Wei C, Briones B, Simmons H, Ibrahim N, Alvarez R, Murray JL, Keyomarsi K, and Moulder S (2015) A phase 1 study with dose expansion of the CDK inhibitor dinaciclib (SCH 727965) in combination with epirubicin in patients with metastatic triple negative breast cancer. *Invest New Drugs* **33**:890–894.
- O’Leary B, Finn RS, and Turner NC (2016) Treating cancer with selective CDK4/6 inhibitors. *Nat Rev Clin Oncol* **13**:417–430.
- Pauwels B, Wouters A, Peeters M, Vermorken JB, and Lardon F (2010) Role of cell cycle perturbations in the combination therapy of chemotherapeutic agents and radiation. *Future Oncol Lond Engl* **6**:1485–1496.

JPET #257717

- Petersen C, Zips D, Krause M, Schöne K, Eicheler W, Hoinkis C, Thames HD, and Baumann M (2001) Repopulation of FaDu human squamous cell carcinoma during fractionated radiotherapy correlates with reoxygenation. *Int J Radiat Oncol Biol Phys* **51**:483–493.
- Pozo K, Castro-Rivera E, Tan C, Plattner F, Schwach G, Siegl V, Meyer D, Guo A, Gundara J, Mettlach G, Richer E, Guevara JA, Ning L, Gupta A, Hao G, Tsai L-H, Sun X, Antich P, Sidhu S, Robinson BG, Chen H, Nwariaku FE, Pfragner R, Richardson JA, and Bibb JA (2013) The role of Cdk5 in neuroendocrine thyroid cancer. *Cancer Cell* **24**:499–511.
- Prevo R, Pirovano G, Puliyadi R, Herbert KJ, Rodriguez-Berriguete G, O’Docherty A, Greaves W, McKenna WG, and Higgins GS (2018) CDK1 inhibition sensitizes normal cells to DNA damage in a cell cycle dependent manner. *Cell Cycle Georget Tex* **17**:1513–1523.
- Romano G, and Giordano A (2008) Role of the cyclin-dependent kinase 9-related pathway in mammalian gene expression and human diseases. *Cell Cycle Georget Tex* **7**:3664–3668.
- Santamaría D, Barrière C, Cerqueira A, Hunt S, Tardy C, Newton K, Cáceres JF, Dubus P, Malumbres M, and Barbacid M (2007) Cdk1 is sufficient to drive the mammalian cell cycle. *Nature* **448**:811–815.
- Satyanarayana A, and Kaldis P (2009) Mammalian cell-cycle regulation: several Cdks, numerous cyclins and diverse compensatory mechanisms. *Oncogene* **28**:2925–2939.
- Sawai CM, Freund J, Oh P, Ndiaye-Lobry D, Bretz JC, Strikoudis A, Genesca L, Trimarchi T, Kelliher MA, Clark M, Soulier J, Chen-Kiang S, and Aifantis I (2012) Therapeutic targeting of the cyclin D3:CDK4/6 complex in T cell leukemia. *Cancer Cell* **22**:452–465.
- Sharma RA, Plummer R, Stock JK, Greenhalgh TA, Ataman O, Kelly S, Clay R, Adams RA, Baird RD, Billingham L, Brown SR, Buckland S, Bulbeck H, Chalmers AJ, Clack G, Cranston AN, Damstrup L, Ferraldeschi R, Forster MD, Golec J, Hagan RM, Hall E, Hanauske A-R, Harrington KJ, Haswell T, Hawkins MA, Illidge T, Jones H, Kennedy AS, McDonald F, Melcher T, O’Connor JPB, Pollard JR, Saunders MP, Sebag-Montefiore D, Smitt M, Staffurth J, Stratford IJ, Wedge SR, and NCRI CTRad Academia-Pharma Joint Working Group (2016)

JPET #257717

- Clinical development of new drug-radiotherapy combinations. *Nat Rev Clin Oncol* **13**:627–642.
- Sherr CJ, Beach D, and Shapiro GI (2016) Targeting CDK4 and CDK6: From Discovery to Therapy. *Cancer Discov* **6**:353–367.
- Syn NL, Lim PL, Kong LR, Wang L, Wong AL, Lim CM, Loh TKS, Siemeister G, Goh BC and Hsieh WS (2018) Pan-CDK inhibition augments cisplatin lethality in nasopharyngeal carcinoma cell lines and xenograft models. *Signal Transduct Target Ther* **3**:9.
- Terasima T, and Tolmach LJ (1963) Variations in several responses of HeLa cells to x-irradiation during the division cycle. *Biophys J* **3**:11–33.
- Whittaker SR, Mallinger A, Workman P, and Clarke PA (2017) Inhibitors of cyclin-dependent kinases as cancer therapeutics. *Pharmacol Ther* **173**:83–105.
- Wu CX, Wang XQ, Chok SH, Man K, Tsang SHY, Chan ACY, Ma KW, Xia W, and Cheung TT (2018) Blocking CDK1/PDK1/ β -Catenin signaling by CDK1 inhibitor RO3306 increased the efficacy of sorafenib treatment by targeting cancer stem cells in a preclinical model of hepatocellular carcinoma. *Theranostics* **8**:3737–3750.
- Xia Q, Cai Y, Peng R, Wu G, Shi Y, and Jiang W (2014) The CDK1 inhibitor RO3306 improves the response of BRCA-proficient breast cancer cells to PARP inhibition. *Int J Oncol* **44**:735–744.
- Yaromina A, Kroeber T, Meinzer A, Boeke S, Thames H, Baumann M, and Zips D (2011) Exploratory study of the prognostic value of microenvironmental parameters during fractionated irradiation in human squamous cell carcinoma xenografts. *Int J Radiat Oncol Biol Phys* **80**:1205–1213.
- Ye X, Zhu C, and Harper JW (2001) A premature-termination mutation in the *Mus musculus* cyclin-dependent kinase 3 gene. *Proc Natl Acad Sci U S A* **98**:1682–1686.

JPET #257717

Footnotes

Financial support: This work was supported by the National Research Foundation of Korea [Grant No. NRF-2017M2A2A7A01019214] and the Korea Institute of Radiological and Medical Sciences, funded by Ministry of Science and ICT, Republic of Korea [Grant No. 50531-2018].

Figure Legends

Fig 1. N-phenylpyrimidin-2-amine (PPA) derivatives can induce G2/M arrest. (A) Cell viability of A549 cells at 72 h after treatment with 10 μ M PPAs. Data are shown as the means \pm SD of three independent experiments. * $P < 0.05$, ** $P < 0.01$, and *** $P < 0.001$. (B) A549 cells were treated with 10 μ M PPAs for 72 h and then subjected to cell cycle analysis. Data represent the mean of each cell cycle population from three independent experiments. (C) Histograms of selected PPA compounds based on one representative result of (B). M1: sub-G1 phase; M2: G0/G1 phase; M3: S phase; M4: G2/M phase, M5: aneuploid cells.

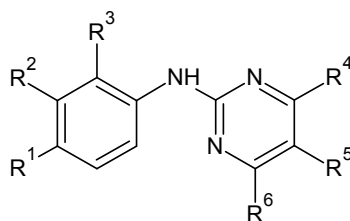
Fig 2. Selected N-phenylpyrimidin-2-amine (PPA) compounds increase radiosensitivity. (A) Cells were treated with the indicated PPAs (10 μ M) for 24 h prior to a 5 Gy dose of γ -irradiation and subjected to cell cycle analysis after further incubation for 24 h. One representative result from three independent experiments is shown. M1: sub-G1 phase; M2: G0/G1 phase; M3: S phase; M4: G2/M phase, M5: aneuploid cells. (B) A549 cells were treated with 1 μ M PPAs for 24 h and then exposed to a 3.5 Gy dose of irradiation. Cells were stained with methylene blue 10 days after irradiation, and representative staining images are shown. (C) Surviving fractions of the cells from (B), as an indicator of radiosensitivity. Data are shown as the mean \pm SD of the normalized values for each drug alone treatment group. * $P < 0.05$ and ** $P < 0.01$.

Fig 3. N-phenylpyrimidin-2-amine (PPA) compounds modulate cell cycle-related protein expression. (A) A549 and (B) H1299 cells were treated with the indicated PPA at 10 μ M for 48 h. The levels of the indicated proteins were determined with western blotting and quantified by densitometry using Image J software. One representative result of three independent experiments is shown. The intensities of phosphorylated proteins were normalized by the level of their correspondent total proteins and the intensities of other proteins were normalized by the level of β -actin. Values are given as the mean \pm SD from three independent experiments. * $P < 0.05$, ** $P < 0.01$, and *** $P < 0.001$.

JPET #257717

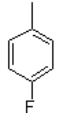
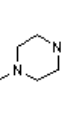
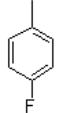
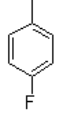
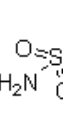
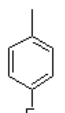
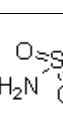
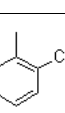
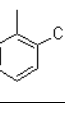
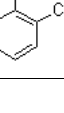
Fig 4. N-Phenylpyrimidine-2-amine (PPA) derivative PPA15 promotes radiosensitivity *in vitro* and *in vivo*. A549 and H1299 cells were treated with 10 μ M PPA15 for 24 h, following treatment with or without a 5 Gy dose of γ -radiation. (A) After 24 h, quantitative analysis of apoptosis was conducted with the annexin V/PI assay using flow cytometry. Data are shown as mean \pm SD of annexin-positive cells from three independent experiments. (B) The levels of the apoptosis-related proteins were determined by western blotting. One representative image from three independent experiments is shown. Values are expressed as the mean \pm SD from three independent experiments. (C) A549 (1×10^6) cells were injected subcutaneously into the thigh hind leg of nude mice (n = 4 mice/group). One week after tumor cell injection, either PPA5 (10 mg/kg) or PPA15 (2 mg/kg) was administered intraperitoneally 24 h prior to local γ -radiation at a dose of 5 Gy. Data are shown as the mean \pm SE of tumor volume. The red and blue markers represent the statistical significance of PPA15 and PPA5, respectively. (D) Cells from several tumor types were treated with 1 μ M PPA15 for 24 h and exposed to a 3 Gy dose of γ -radiation. Surviving clonal cells were visualized at 10–14 days after irradiation. One representative result from three independent experiments is shown. * $P < 0.05$, ** $P < 0.01$, *** $P < 0.001$ vs. control; † $P < 0.05$, †† $P < 0.01$, ††† $P < 0.001$ vs. IR; ## $P < 0.01$, ### $P < 0.001$ vs. drug alone.

Table 1. Structure of N-phenylpyrimidin-2-amine analogs



derivatives	R1	R2	R3	R4	R5	R6	IUPAC Name
PPA1	-	-		-	-		4-(4-fluorophenyl)-N-phenylpyrimidin-2-amine (ChemBridge, 9227565)
PPA2	-OCH ₃	-		-	-		N-(4-methoxyphenyl)-4-phenylpyrimidin-2-amine (ChemBridge, 9223502)
PPA3	-	-		-	-		N-phenyl-4-(pyridine-2-yl)pyrimidin-2-amine (ChemBridge, 9201661)
PPA4	-NO ₂	-					6-chloro-N-(4-nitrophenyl)-4-phenylquinazolin-2-amine (ChemBridge, 5808624)
PPA5	-NO ₂	-			-		4-(4-fluorophenyl)-N-(4-nitrophenyl)-6-phenylpyrimidin-2-amine (ChemBridge, 5469711)
PPA6	-NH-CO-CH ₃	-		-CH ₃	-		N-(4-((4-methyl-6-(phenylamino)pyrimidin-2-yl)amino)phenyl)acetamide (ChemDiv, G869-0095)
PPA7	-						(3-((6-chloro-4-phenylquinazolin-2-yl)amino)phenyl)((morpholino)methane (ChemBridge, 5960675)
PPA8	-COO-C ₂ H ₅	-			-		Ethyl 4-((4-(4-fluorophenyl)-6-phenylpyrimidin-2-yl)amino) benzoate (ChemBridge, 5475712)
PPA9	-NO ₂	-		-	-		4-(4-fluorophenyl)-N-(4-nitrophenyl)pyrimidin-2-amine
PPA10	-	-			-		4-(4-fluorophenyl)-N,6-diphenylpyrimidin-2-amine

JPET #257717

PPA11	-NH- CO- CH ₃	-			-		N-(4-((4-(4-Fluorophenyl)pyrimidin-2-yl)amino)phenyl)acetamide
PPA12		-			-		4-(4-fluorophenyl)-N-(4-(4-methylpiperazin-1-yl)phenyl) pyrimidin-2-amine
PPA13	-CO- NH- CH ₃	-	-OCH ₃		-		4-((4-(4-fluorophenyl)pyrimidin-2-yl)amino)-3-methoxy-N-methyl benzamide
PPA14		-			-		4-((4-(4-fluorophenyl)pyrimidin-2-yl)amino)benzenesulfonamide
PPA15		-			-		4-((4-(2-chlorophenyl)pyrimidin-2-yl)amino)benzenesulfonamide
PPA16	-	-NO ₂			-		4-(2-chlorophenyl)-N-(3-nitrophenyl)pyrimidin-2-amine
PPA17	-CO- NH- CH ₃	-			-		4-((4-(2-chlorophenyl)pyrimidin-2-yl)amino)-N-methylbenzamide

JPET #257717

Table 2. Kinase inhibitory effects of the N-phenylpyrimidin-2-amin (PPA) derivatives, PPA5 and PPA15.

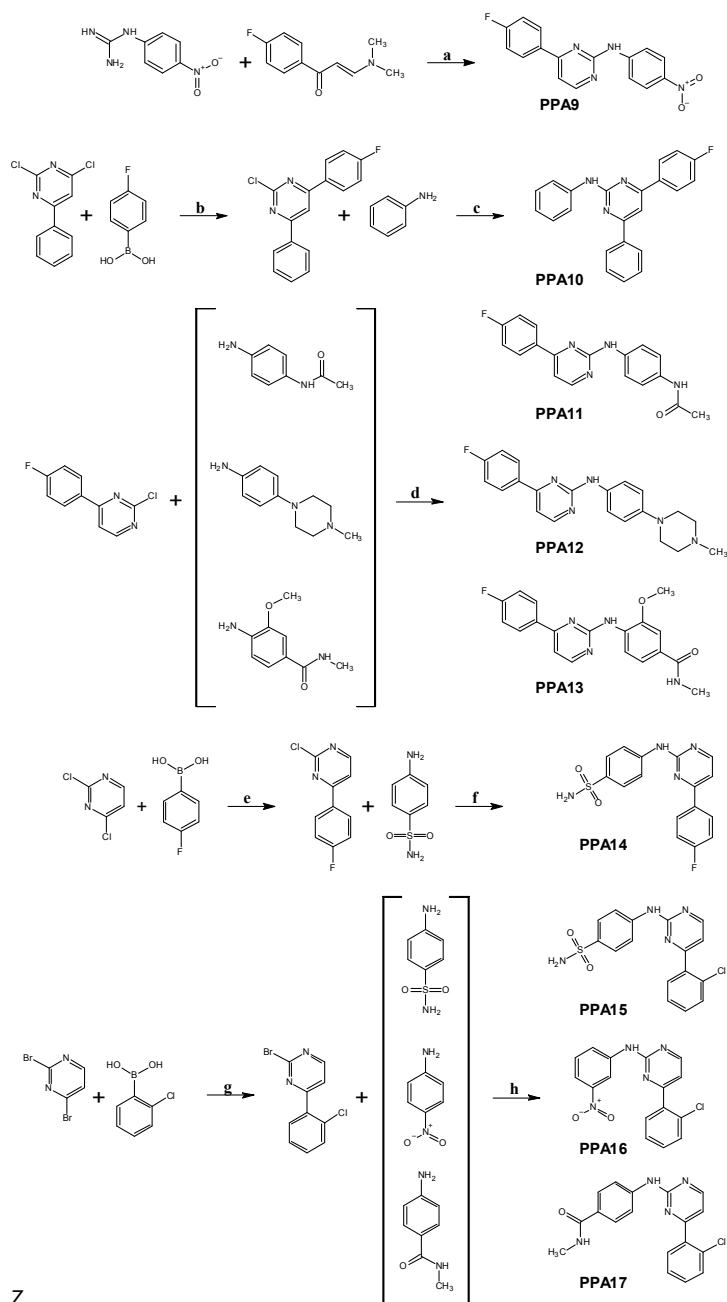
Kinases	Kinase activity (%)	
	PPA5 (10 μ M)	PPA15 (10 μ M)
Aurora-A	103.32 \pm 9.785	2.16 \pm 0.69
Aurora-B	109.57 \pm 2.997	1.14 \pm 0.363
Aurora-C	116.56 \pm 6.718	14.89 \pm 3.308
CDK1/cyclin B	96.84 \pm 6.506	-0.66 \pm 0.526
CDK2/cyclin A	88.08 \pm 1.61	0.61 \pm 0.000
CDK2/cyclin E	92.25 \pm 6.273	-1.67 \pm 0.074
CDK3/cyclin E	89.91 \pm 7.894	-0.08 \pm 0.057
CDK4/cyclin D3	97 \pm 1.449	8.4 \pm 2.752
CDK5/p25	89.84 \pm 6.544	0.5 \pm 1.589
CDK5/p35	101.66 \pm 1.411	0.73 \pm 0.693
CDK6/cyclin D3	99.34 \pm 4.545	6.06 \pm 0.977
CDK7/cyclin H/MAT1	101.78 \pm 0.406	19.89 \pm 2.392
CDK9/cyclin T1	94.9 \pm 3.752	1.24 \pm 0.115
CHK1	105.62 \pm 0.864	81.76 \pm 1.968
CHK2	97.26 \pm 4.61	64.19 \pm 3.172
Plk1	109.06 \pm 1.546	-
Plk3	108.67 \pm 1.274	95.7 \pm 5.397
Wee1	99.22 \pm 3.125	86.53 \pm 6.204
ATM	92.77 \pm 1.411	91.8 \pm 0.276
ATR/ATRIP	97.31 \pm 7.598	93.16 \pm 8.725
DNA-PK	92.17 \pm 2.746	74.93 \pm 1.276

JPET #257717

Table 3. IC₅₀ values of PPA15 activity against a panel of cyclin-dependent kinases (CDKs).

Kinase	IC₅₀ (nM)
CDK1/cyclin B	53
CDK2/cyclin A	19
CDK2/cyclin E	12
CDK3/cyclin E	18
CDK4/cyclin D3	4169
CDK5/p25	9
CDK5/p35	16
CDK6/cyclin D3	1685
CDK7/cyclin H/MAT1	> 10,000
CDK9/cyclin T1	105
CHK1	> 10,000
CHK2	> 10,000

JPET #257717



Z

Scheme 1. Synthesis of N-phenylpyrimidin-2-amine (PPA) derivatives; a = NaOH, isopropanol (IPA), reflux; b = Pd(OAc)₂, Na₂CO₃, PPh₃, THF/H₂O, 60°C; c = Pd(OAc)₂, Cs₂CO₃, 2,2'-bis(diphenylphosphino)-1,1'-binaphthyl (BINAP), dioxane, 100°C; d = Pd(OAc)₂, Cs₂CO₃, BINAP, dioxane, 100°C; e = Pd(PPh₃)₄, K₂CO₃, PhMe/EtOH/H₂O, 60°C; f = Pd₂(dba)₃, K₂CO₃, Xphos, t-BuOH, reflux; g = Pd(PPh₃)₄, K₂CO₃, PhMe/EtOH/H₂O, 60°C; h = Pd₂(dba)₃, K₂CO₃, Xphos, t-BuOH, reflux.

JPET #257717

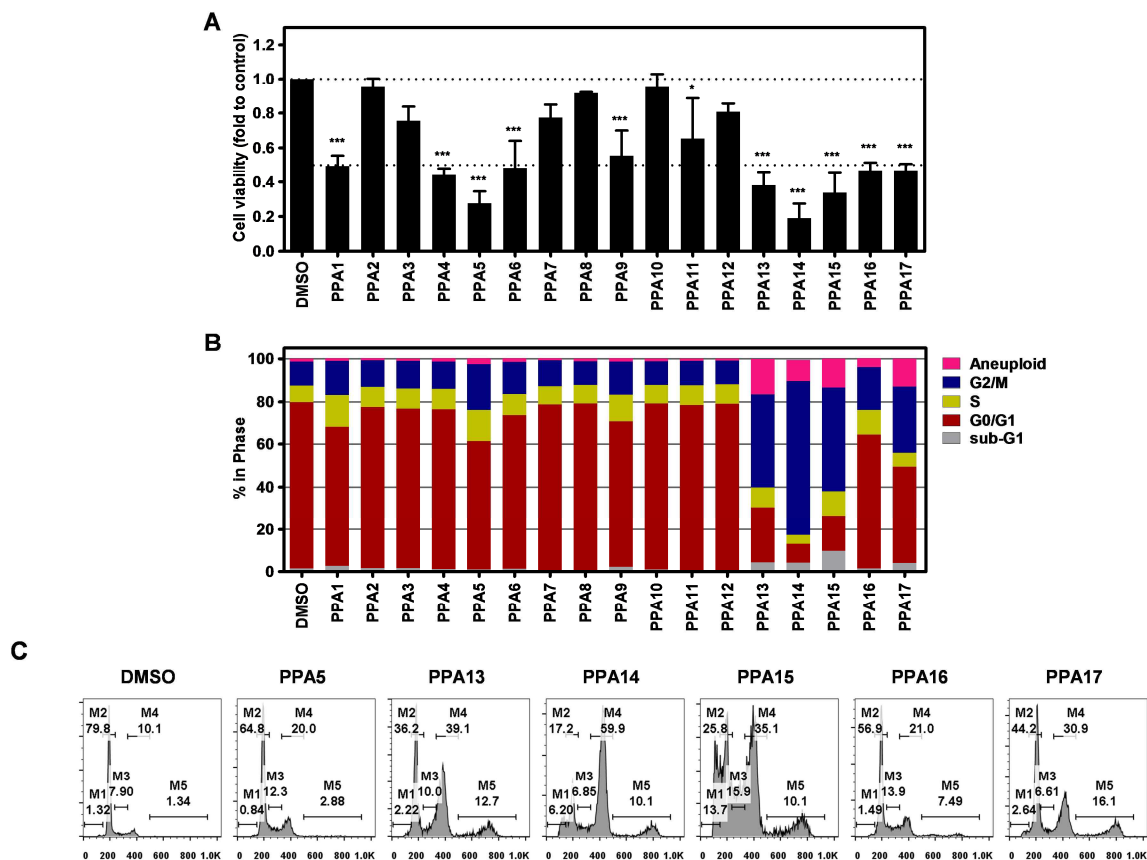


Figure 1.

JPET #257717

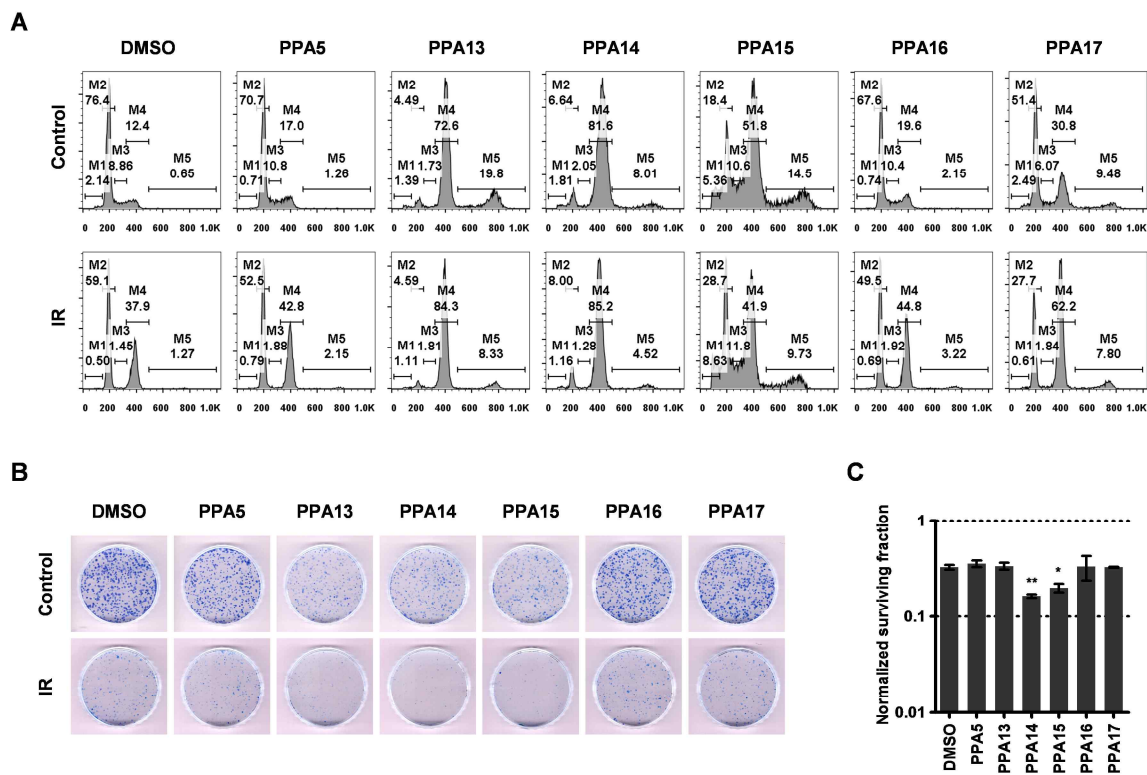


Figure 2.

JPET #257717

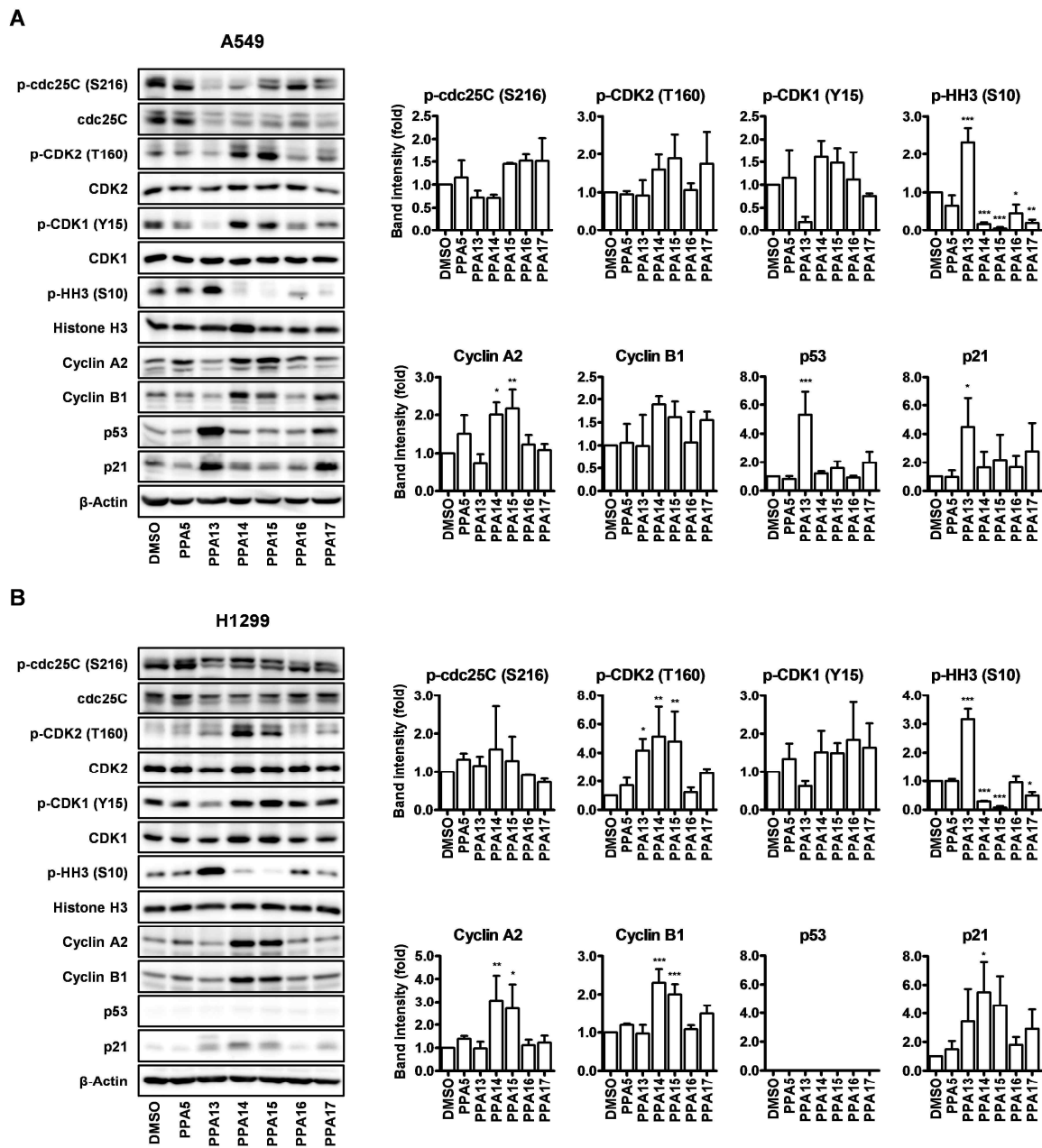
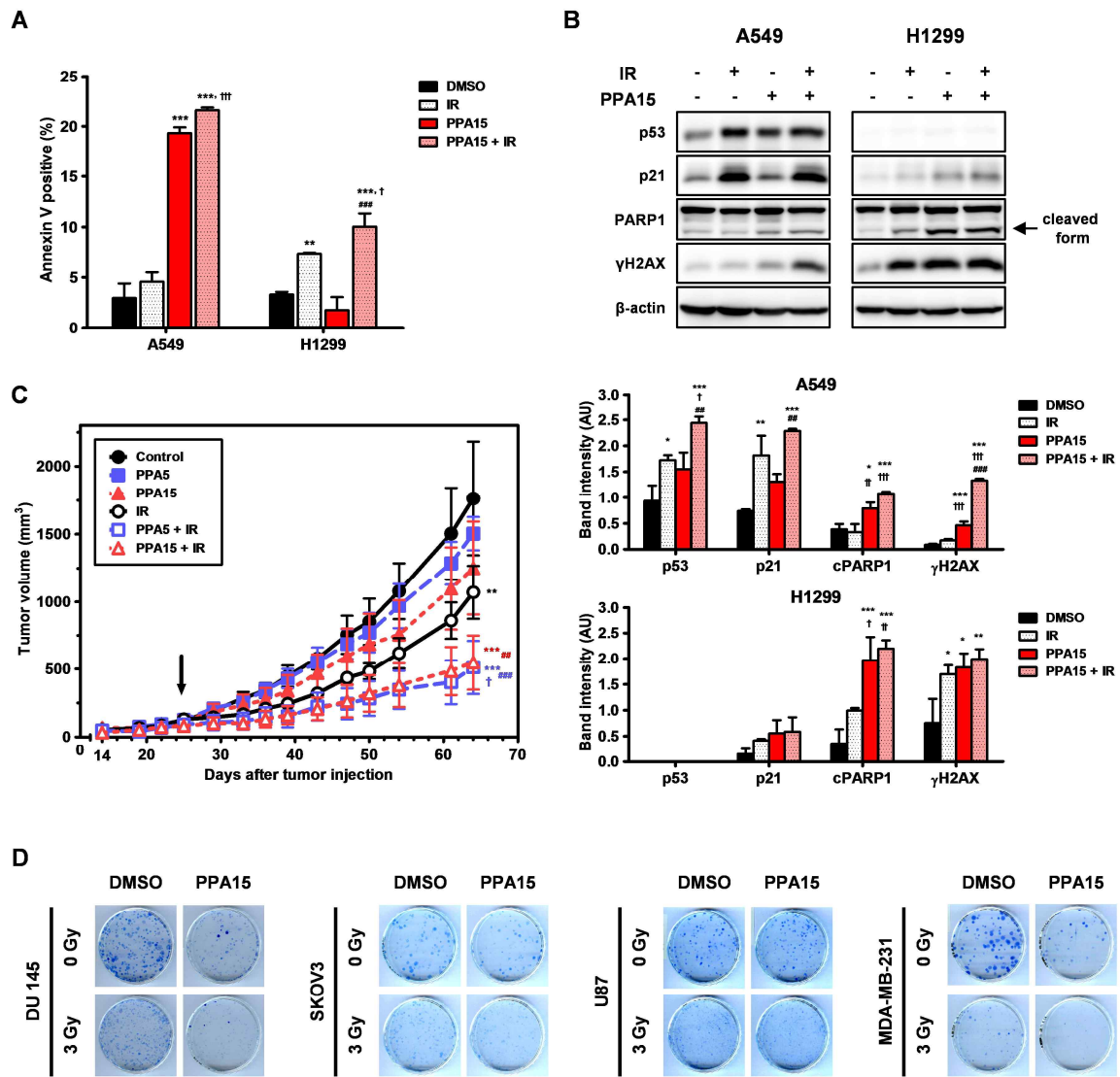


Figure 3.

JPET #257717



**Radiosensitizing effect of novel phenylpyrimidine derivatives on human lung cancer
cells via cell cycle perturbation**

Seung-Youn Jung, Ky-Youb Nam, Jeong-In Park, Kyung-Hee Song, Jiyeon Ahn, Jong Kuk Park,
Hong-Duck Um, Sang-Gu Hwang, Sang Un Choi and Jie-Young Song*

Journal of Pharmacology and Experimental Therapeutics

Supplemental Table 1. Cell cycle profiles of A549 cells treated with N-phenylpyrimidin-2-amine (PPA) derivatives. A549 cells were seeded in 6-well plates and treated with 10 μ M PPAs for 72 h. Cells were then fixed in 70% ethanol and stained with PI for flow cytometry analysis. Data are given as the percentage of cells in each cell cycle phase and show the mean \pm SD from three independent experiments. $**P < 0.01$, $***P < 0.001$ vs. control

Supplemental Table 2. Cell cycle profiles of A549 cells treated with N-phenylpyrimidin-2-amine (PPA) derivatives combined with IR. Cells were treated with the indicated PPAs (10 μ M) for 24 h prior to a 5 Gy dose of γ -irradiation and subjected to cell cycle analysis after further incubation for 24 h. Cells were then fixed in 70% ethanol and stained with PI for flow cytometry analysis. Data are given as the percentage of cells in each cell cycle phase and show the mean \pm SD from three independent experiments. $*P < 0.05$, $**P < 0.01$, $***P < 0.001$ vs. control; $\#P < 0.05$, $\#\#P < 0.01$, $\#\#\#P < 0.001$ vs. drug alone.

Supplemental Fig. 1. Clonogenic survival assay of cancer cells treated with PPA15. DU 145 prostate, SKOV3 cervical, U-87 glioma, and MDA-MB-231 breast cancer cells were treated with PPA15 (1 μ M) 24 h after seeding, and cells were irradiated with the indicated doses of γ -radiation 24 h later. Colonies were stained after 10–14 days. One representative result of three independent experiments is shown. Visible colonies were manually counted, and the survival fractions were calculated. The survival fractions of three independent experiments were represented as the mean \pm SD, and the survival curve was fitted with Linear-Quadratic (LQ) model by using GraphPad Prism 5 Software.

Supplemental Table 1.

	sub-G1	G0/G1	S	G2/M	Aneuploid
DMSO	1.45 ± 0.44	78.40 ± 3.05	7.68 ± 4.83	11.14 ± 2.23	1.43 ± 0.50
PPA1	2.69 ± 2.46	65.67 ± 5.33	14.80 ± 6.37	15.87 ± 2.634	1.13 ± 0.32
PPA2	1.65 ± 0.42	75.93 ± 4.43	9.39 ± 5.683	12.27 ± 1.42	0.88 ± 0.36
PPA3	1.62 ± 0.24	75.17 ± 4.42	9.37 ± 5.84	12.87 ± 1.16	1.06 ± 0.43
PPA4	1.22 ± 0.24	75.27 ± 6.74	9.52 ± 6.49	12.73 ± 0.32	1.42 ± 0.17
PPA5	1.05 ± 0.76	60.27 ± 3.99	14.93 ± 3.28	21.30 ± 2.88	2.68 ± 0.24
PPA6	1.29 ± 1.12	72.50 ± 2.50	9.90 ± 4.50	14.80 ± 1.65	1.63 ± 0.47
PPA7	0.82 ± 0.23	78.07 ± 4.42	8.28 ± 4.77	12.07 ± 0.47	0.87 ± 0.14
PPA8	0.74 ± 0.26	78.47 ± 4.86	8.60 ± 5.10	11.03 ± 0.49	1.24 ± 0.19
PPA9	2.35 ± 2.30	68.63 ± 9.71	12.34 ± 8.64	15.30 ± 2.96	1.52 ± 0.44
PPA10	0.96 ± 0.22	78.27 ± 4.58	8.56 ± 4.56	11.10 ± 0.36	1.19 ± 0.31
PPA11	0.61 ± 0.21	77.87 ± 2.27	9.29 ± 4.38	11.23 ± 2.05	1.03 ± 0.26
PPA12	0.63 ± 0.21	78.40 ± 3.52	9.14 ± 5.28	10.98 ± 1.76	0.93 ± 0.21
PPA13	4.40 ± 1.94	26.01 ± 15.78***	9.40 ± 2.75	43.67 ± 9.60***	16.40 ± 7.20***
PPA14	4.18 ± 2.32	8.96 ± 7.24***	4.17 ± 2.35	72.43 ± 10.96***	9.77 ± 1.33**
PPA15	9.83 ± 3.57***	16.75 ± 8.92***	11.43 ± 5.50	48.67 ± 14.02***	13.37 ± 2.87***
PPA16	1.57 ± 0.82	62.80 ± 5.37	11.83 ± 3.51	20.03 ± 1.00	4.01 ± 3.01
PPA17	4.12 ± 2.36	45.27 ± 3.14***	6.49 ± 2.10	31.20 ± 1.57***	13.02 ± 3.12***

Supplemental Table 2.

	sub-G1	G0/G1	S	G2/M	Aneuploid
DMSO	1.29 ± 0.93	73.90 ± 4.24	9.15 ± 0.69	15.20 ± 4.02	0.79 ± 0.23
PPA5	1.20 ± 0.91	67.87 ± 4.65	10.73 ± 0.60	19.13 ± 3.03	1.41 ± 0.13
PPA13	1.76 ± 1.50	3.44 ± 1.08 ^{***}	2.50 ± 0.87 ^{**}	67.03 ± 7.13 ^{***}	25.30 ± 6.06 ^{***}
PPA14	2.32 ± 1.26	7.20 ± 0.88 ^{***}	5.04 ± 5.42	74.23 ± 12.93 ^{***}	10.42 ± 3.89
PPA15	4.96 ± 1.26	16.87 ± 3.01 ^{***}	10.97 ± 0.40	54.57 ± 6.23 ^{***}	13.17 ± 2.66
PPA16	0.86 ± 0.28	65.00 ± 4.77	10.49 ± 0.57	21.57 ± 3.24	2.41 ± 0.49
PPA17	2.49 ± 0.03	48.13 ± 4.98 ^{***}	6.08 ± 0.48	33.93 ± 5.34	9.52 ± 0.16
IR + DMSO	0.42 ± 0.09	53.23 ± 9.82 ^{###}	3.34 ± 3.26 [#]	41.10 ± 5.29 [#]	1.57 ± 0.47
IR + PPA5	1.43 ± 1.14	47.97 ± 7.17 ^{###}	2.54 ± 0.98 ^{###}	45.93 ± 5.09 [#]	2.25 ± 0.14
IR + PPA13	1.04 ± 0.74	2.69 ± 1.65 ^{***}	1.77 ± 0.61	78.53 ± 13.23 ^{***}	16.01 ± 13.77 [*]
IR + PPA14	3.21 ± 3.67	11.26 ± 4.99 ^{***}	3.31 ± 3.79	75.93 ± 15.96 ^{**}	5.58 ± 2.14
IR + PPA15	7.60 ± 1.41 ^{***}	26.93 ± 2.72 ^{***}	12.57 ± 1.50 ^{***}	45.60 ± 5.16	7.81 ± 2.98
IR + PPA16	0.87 ± 0.32	44.70 ± 8.14 ^{###}	2.61 ± 0.83 ^{###}	48.53 ± 7.08 [#]	3.39 ± 0.26
IR + PPA17	1.13 ± 0.81	24.33 ± 5.66 ^{***, ###}	2.61 ± 1.28	64.90 ± 4.42 ^{##}	7.11 ± 0.99

Supplemental Figure 1.

